EZH2 represses mesenchymal genes and upholds epithelial identity in breast cancer cells

Amador Gallardo [1,2,3], Efres Belmonte-Reche [1,2,3], Aldara Molina [1,2,3] and David Landeira [1,2,3]

[1] Centre for Genomics and Oncological Research (GENYO), Avenida de la Ilustración 114, 18016 Granada, Spain

[2] Department of Biochemistry and Molecular Biology II, Faculty of Pharmacy, University of Granada, Granada, Spain

[3] Instituto de Investigación Biosanitaria ibs.GRANADA, Hospital Virgen de las Nieves, Granada, Spain

Correspondence to David Landeira: davidlandeira@ugr.es

Running title: EZH2 upholds epithelial identity in breast cancer cells.

Keywords: Epigenetics, Polycomb, EZH2, EMT, MET, cell plasticity, breast cancer.

Summary

Emerging studies support that the Polycomb Repressive Complex 2 (PRC2) regulates phenotypic changes of cancer cells by modulating their shifts among metastable states within the epithelial and mesenchymal spectrum. This new role of PRC2 in cancer has been recently proposed to stem from the ability of its catalytic subunit EZH2 to bind and modulate the transcription mesenchymal genes during epithelial-mesenchymal transition (EMT) in lung cancer cells. Here, we asked whether this mechanism is conserved across different types of carcinomas. By combining TGF-β-mediate reversible induction of epithelial to mesenchymal transition and pharmacological inhibition of EZH2 activity we demonstrate that EZH2 represses a large set of mesenchymal genes and favours the residence of breast cancer cells towards the more epithelial spectrum during EMT. In agreement, analysis of human patient samples support that EZH2 is required to efficiently repress mesenchymal genes in breast cancer tumours. Our results indicate that PRC2 operates through similar mechanisms in breast and lung cancer cells, supporting that PRC2-mediated direct transcriptional modulation of the mesenchymal gene expression program is a conserved molecular mechanism underlying cell dissemination across human carcinomas.

Introduction

Polycomb group (PcG) proteins are hallmark epigenetic regulators of embryo development, stem cell differentiation and cancer [3, 24, 26]. PcG proteins associate to form multimeric complexes termed Polycomb Repressive Complexes 1 and 2 (PRC1 and PRC2) that can post-translationally modify histone tails and repress gene transcription. RING1A/B is the catalytic subunit of PRC1 and monoubiquitinates lysine 119 on histone H2A (H2AK119ub). Likewise, EZH1/2 harbours the catalytic activity of PRC2 and trimethylates lysine 27 on histone H3 (H3K27me3). The coordinated activity of PRCs leads to the formation of chromatin domains enriched in H2AK119ub and H3K27me3 that facilitate transcriptional repression of hundreds of genes across the genome in a cell-type-specific manner.

In stem cells, the activity of PRCs lead to the transcriptional repression of hundreds of lineage-inappropriate genes, contributing to maintain a specific gene expression program and define stem cell identity [3, 24, 26]. In the context of cancer, initial studies revealed that PcG proteins act as oncogenes through the transcriptional repression of the *INK4A/ARF* (*CDKN2A*) tumour suppressor locus [4, 12]. However, subsequent studies confirmed that this was just one aspect of the role of PRC in cancer, because different PRC subunits can have senescence-independent prooncogenic activity or tumour suppressor function [24, 27]. In fitting with its role as a regulator of cell identity in stem cell biology, recent studies support that PRC2 can regulate dynamic phenotypic changes of cancer cells by modulating their transition between metastable states within the epithelial and mesenchymal spectrum through poorly understood mechanisms [9, 27, 28, 34]. Reversible transition between the epithelial and mesenchymal states vertebrate carcinoma cell dissemination [17], and inhibitors of the PRC2 catalytic subunits EZH2 are currently being developed to treat several types of carcinomas [15]. Therefore, understanding the molecular basis of the function of PRC2 in EMT is crucial for a precise understanding of the molecular basis of cancer dissemination, and for safe application of PRC inhibitors in the clinics.

PRC2 activity modulates the epithelial state of lung and breast carcinoma cells [9, 27-29, 34]. Thus, loss of function of PRC2 subunits EZH2 or EED leads to acquisition of mesenchymal features and changes in tumour colonization capacity [9, 27-29, 34]. This effect has been recently proposed to stem from the ability of EZH2 to directly bind the gene promoter regions and modulate the transcription of a large set of mesenchymal genes through H3K27me3 during epithelial to mesenchymal transition (EMT) in lung cancer cells [9]. Here, we asked whether direct regulation of the mesenchymal gene expression program by PRC2 is a specific feature of lung cancer cells or whether it is a conserved mechanism also present in other types of carcinoma cells. We found that EZH2 repress a large set of mesenchymal genes and promotes the residence of breast cancer cells in a more mesenchymal state. We propose that direct transcriptional modulation of the mesenchymal gene expression program by PRC2 is a conserved molecular mechanism across different types of carcinomas that endorses cells with the plasticity required for efficient cell dissemination.

Results

EZH2 represses bivalent mesenchymal genes in breast carcinoma cells.

To analyse the function of EZH2 in breast cancer we focused on the human MCF-7 cell line because it is a well-stablished system to study the molecular basis of breast cancer. These cells are homozygous null mutant for the *CDKN2A* locus, which makes them a good model to study the *CDKN2A*-independent function of EZH2 in cancer. We first set to identify what genes are directly regulated by EZH2 in MCF-7 cells. EZH2 catalyses H3K27me3 at the promoter regions of target genes, and thus, the genome-wide distribution of H3K27me3 is a surrogate measure of EZH2 binding [3, 5]. Analysis of H3K27me3 binding maps revealed that EZH2 target the promoter region of 5175 genes in MCF-7 cells (Figure 1A). In pluripotent cells, many H3K27me3-repressed target genes display chromatin features of active transcription such as trimethylation of H3K4

(H3K4me3) and they are usually referred to as bivalent genes [21]. Bivalent chromatin seems to facilitate their transcriptional activation during lineage transition [21]. Interestingly, comparison of H3K27me3 and H3K4me3 genome-wide binding maps in MCF-7 cells revealed that 1015 genes (19.6%) out of the 5175 genes marked by H3K27me3 displayed a bivalent state, and hence they accumulated both modifications at their promoter region (Figure 1A, B). Importantly, bivalent genes were enriched for genes involved in the regulation of mesenchymal features, EMT and KRAS signalling, and included genes that are widely used as mesenchymal markers such as *N-CADHERIN* and *SNAI2* (Figure 1C, 1D, S1A). Thus, we concluded that in MCF-7 cells, EZH2 binds a large set of mesenchymal genes that display features of bivalent chromatin. We hypothesized that this bivalent state might facilitate the coordinated transcriptional activation of mesenchymal genes in response to signalling molecules during EMT.

To address whether EZH2 is repressing the mesenchymal gene expression program through H3K27me3 in breast cancer cells, we treated MCF-7 cells with a highly specific small molecule that inhibits EZH2 methyltransferase activity (GSK126, thereafter referred to as EZH2i) [22] and analyse whether the loss of H3K27me3 induced the activation of the mesenchymal program. Inhibition of EZH2 led to a drastic expected reduction of global levels of H3K27me3 (Figure 1E), and only mild inhibition of cell proliferation that did not impair long-term culture of MCF-7 cells (Figure S1B). Importantly, reduced levels of H3K27me3 during 12 days of culture led to a remarkable transcriptional activation of the mesenchymal marker *N-CADHERIN* (Figure 1F), which is a H3K27me3-positive direct target of EZH2 (Figure S1A). Likewise, analysis of the expression of master EMT transcription factors (EMT-TFs) (SNAI1/2, TWIST1/2 and ZEB1/2) revealed an evident specific activation of the *SNAI2* gene (Figure 1G, 1H), which was the only EMT-TF that was directly targeted by EZH2 (Figure S1A). As expected, activation of mesenchymal genes upon EZH2 inhibition led to downregulation of epithelial marker *E-CADHERIN* (Figure S1C, S1D). Importantly, activation of mesenchymal genes in MCF-7 cells upon depletion of H3K27me3 was functionally relevant because cells treated with EZH2i displayed obvious increased mobility compared to untreated cells in cultured wound healing assay (Figure 1I). Thus, we concluded that EZH2 target and repress the transcription of a large set of bivalent mesenchymal genes in the breast cancer cell line MCF-7.

To confirm that EZH2 functions as a gatekeeper of epithelial identity in breast cancer cells we analysed whether inhibition of EZH2 led to the transcriptional activation of mesenchymal genes in cell lines derived from different types of metastatic breast adenocarcinomas: MCF7 cells (ER+/PR+-/Her2-), SKBR3 cells (ER-, PR-, Her2+) and MDA-MB-231 cells (ER-/PR-/Her2-). Cells were plated at low density to form colonies during 14 days in the presence of EZH2i. Inhibition of EZH2 induced minor effects on cell growth (Figure S1E), confirming the suitability of these cell lines to study the proliferation-independent role of EZH2. EZH2i-treated cells displayed unpacked colonies composed by cells with more elongated and fusiform morphology typically associated with the mesenchymal state, as compared to non-treated control cultures composed of cells with a more epithelial appearance (Figure S1F). In agreement, inhibition of EZH2 activity induced the expression of different combinations of well-established mesenchymal genes such as *SNAI1/2*, *TWIST1/2*, *ZEB1/2* or *MMP2* in the three different cell lines (Figure 1J). Overall, we concluded that EZH2 is required to maintain the transcriptional repression of mesenchymal genes and to favour an epithelial state in breast cancer cells.

EZH2 is required to repress mesenchymal genes during TGF-β-dependent MET in breast cancer cells.

To directly analyse whether EZH2 regulates transitions between the epithelial and mesenchymal states of breast cancer cells we setup an in vitro system to study the dynamics of EMT and its reverse process (mesenchymal to epithelial transition, MET), as we have previously described for lung cancer cells [9]. Treatment of MCF-7 cells with 10 ng/ml transforming growth factor beta (TGF-β) and 50 ng/ml epidermal growth factor (EGF) during six days induced the transcription of

mesenchymal markers (*N-CADHERIN, NRP2, TWIST1 and SNAI2*) and the downregulation of the epithelial marker *E-CADHERIN* (Figure S2A, S2B). Withdrawal of TGF-β and EGF from the culture media during six additional days led to the reversion of the phenotype: downregulation of the expression of mesenchymal genes (*N-CADHERIN, NRP2, TWIST1 and SNAI2*) coupled to activation of the epithelial marker E-CADHERIN (Figure S2A, S2B). Importantly, changes in the expression of epithelial and mesenchymal genes were accompanied by expected functional changes in cell mobility in cultured wound healing assays (Figure S2C).

To test whether inhibition of EZH2 alters EMT-MET in MCF-7 cells we compared the expression of epithelial (*E-CADHERIN*) and mesenchymal (*N-CADHERIN, NRP2, TWIST1 and SNAI2*) genes in cells treated or untreated with EZH2i (Figure 2A). Induction of EMT with TGF-β led to an enhanced activation of mesenchymal genes at day 6 as compared to untreated cells (Figure 2B). Importantly, restoration of mesenchymal gene repression upon MET on day 12 was severely hindered in cells in which EZH2 was inhibited (Figure 2B, note the difference in expression of *N-CADHERIN*). In agreement, examination of the in vitro wound healing capacity of MCF-7 cells showed that treatment with EZH2i slightly increased the mobility of cells after six days of EMT (day 6) and hindered the restoration of the more immobile epithelial phenotype upon MET (day 12) (Figure 2C). Therefore, we settled that EZH2 is required to downmodulate the expression of mesenchymal genes during EMT-MET in breast cancer cells, and to allow efficient restoration of the epithelial state during MET.

Expression of *EZH2* inversely correlates with the expression of mesenchymal genes in human breast tumours.

To confirm that EZH2 represses mesenchymal genes in breast cancer cells, we used genome-wide gene expression datasets of 1904 resected breast cancer tumours available at the Molecular Taxonomy of Breast Cancer International Consortium. Importantly, we found that the levels of *EZH2* mRNA inversely correlate with the expression of EZH2 target genes identified in Figure 1A (881 out of the 1015 genes identified in figure 1A were analysable in these datasets) (Figure 3A). Negative correlation was even more obvious for the group of 57 bivalent genes identified as mesenchymal in Figure S1A (Figure 3A). As expected, no significant correlation was found for a group of randomly selected control genes (Figure 3A). The expression values of individual mesenchymal genes such as *SNAI2* also displayed the expected negative correlation (Figure3B). Therefore, these analyses support that EZH2 functions as a transcriptional repressor of the mesenchymal gene expression program in human breast cancer tumours. In agreement with previous reports [1, 13], high expression of *EZH2* was associated with poor survival probability in our patient cohort (median survival, high: 132.3 months, low: 172.9 months) (Figure 3C). Thus, we concluded that augmented expression of EZH2 is associated to reduced expression of EZH2-target mesenchymal genes in breast cancer tumours and that high levels of EZH2 expression are associated with poor survival.

Discussion

Metastatic processes cause around 90% of cancer-associated mortality and therefore understanding the mechanisms underlying metastatic dissemination is crucial to develop more effective therapies [17]. Metastatic dissemination relies on dynamic changes in cancer cell state that occur during epithelial to mesenchymal reversible transitions [6]. Specifically, emerging reports indicate that cancer malignancy and disease progression rely on the ability of cancer cells to reside in intermediate metastable states within the epithelial – mesenchymal spectrum, rather than in extreme epithelial or mesenchymal states [14, 20, 23, 30]. Epigenetic regulators, rather than genetic mutations, have been proposed to be key regulators of cancer cell plasticity, but the fundamental mechanisms involved remain poorly understood [5-7].

Our study reveals that the PRC2 catalytic subunit EZH2 coordinates the repression of the mesenchymal gene expression program in breast cancer cells, facilitating MET upon TGF-β

stimulation decay. These results explain why EZH2-deficient breast cancer cells display reduced capacity to colonize new organs and form metastasis [11, 32]. The oncogenic activity of EZH2 is further supported by its behaviour as a marker of poor prognosis in breast cancer patients (this study and [2, 13, 16]). Importantly, our observations are in consonance with previous reports studying lung cancer cells, where it has been shown that the loss of function of EZH2 hinders repression of mesenchymal genes during MET [9], and reduces tumour colonization capacity in mouse models [9, 27, 28]. Counterintuitively, it has been recently reported that loss of function of a non-catalytic PRC2 subunit (EED) in experimentally transformed human mammary epithelial cells (HMLER) leads to increased metastasis in mouse xenograft experiments [34]. This apparent discrepancy might rely on variations in EZH2 activity in the different systems: while in our experiments and previous reports the activity of EZH2 protein is reduced to undetectable levels [9, 11, 27, 28, 32], EED-depleted HMLER cells display partial downregulation of EZH2 protein [34]. Based on the discoveries made in the present manuscript, we propose that low activity of EZH2 protein in EED-depleted HMLER cells promote the transition of breast cancer cells into a metastable mesenchymal state without substantially blocking MET, explaining the enhanced tumour colonization capacity of EED mutant cells. Overall, observations presented in this study serve to bring together previous reports in breast [11, 32, 34] and lung cancer cells [9, 27, 28], and support a cell-of-origin-independent role of PRC2 as a direct modulator of the mesenchymal gene expression program during EMT-MET in human carcinomas.

Methods

Breast cancer cell lines culture conditions

The MCF-7, MDA-MB-231, SKBR3 and BT474 cell lines were kindly provided by the labs of Mª Jose Serrano and Dr. Juan Antonio Marchal (University of Granada, Spain). Cells were grown at 5% CO2 and 37 ºC in DMEM high glucose media supplemented with 10% heat inactivated fetal bovine serum (FBS) (Gibco), penicillin/streptomycin (Gibco), L-glutamine (Gibco) and 2-mercaptoethanol (Gibco). Detailed information about cell lines used is provided in supplementary table S1.

Induction of in vitro EMT-MET by TGF-β and EGF stimulation in MCF-7 cells.

Epithelial MCF-7 cells were plated at a density of 10.000 cells/cm^2 and treated with 10 ng/mL TGF-β (Prepotech) and 50 ng/mL EGF (Prepotech) for 6 days to induce transition into a mesenchymal state (EMT). Thereafter, both cytokines were removed from the culture media and cells were grown for 6 additional days to allow reversion to the epithelial state (MET). Cells were trypsinized, counted and replated at initial density in fresh media every 48h.

Treatment of breast cancer cell lines with EZH2 inhibitor

EZH2 was inhibited using 5 µM GSK126 (A3446, APExBIO). Treatments with EZH2 inhibitor for 12 days were carried out by refreshing GSK126 every two days as MCF-7 cells were split to allow exponential cell growth. Likewise, during EMT-MET experiments, GSK126 was refreshed every two days as cells were diluted to the corresponding density (10 000 cells/cm^2). In colony forming assays, cells were pre-treated with GSK126 for 4 days to reduce the global H3K27me3 level before plating the cells. MCF-7, SKBR3 and MDA-MB-231 cells were seed at a density of 200 cells/cm^2 to allow formation of colonies after 14 days. Media was refreshed every 5 days including GSK126 in the treated culture. In growth curves, cell viability and wound healing assays, cells were pre-treated with GSK126 for 4 days to reduce global H3K27me3 levels before the start of the experiment. Cells were maintained in the presence of GSK126 during the experiment as detailed below.

Growth curve, cell viability and in vitro wound healing assays

To perform growth curves cells were platted at density of 10.000 cells/cm^2 and diluted before confluence to the initial density. Accumulative growth was calculated by applying the dilution factor used. Inhibition of EZH2 was carried out by pre-treating cells with GSK126 for four days and refreshing the inhibitor in every cell dilution.

To analyse cell survival cells were pre-treated with GSK126 for 4 days, plated in 96 well plate at a density of 3000 cells per well and allowed to grow. After 48h, cell media was replaced by fresh media containing 0.1mM of resazurin. The plate was incubated for 4h at 37ºC and fluorescence at 585 nm wavelength was measured. Same procedure was applied to GSK126 untreated control cells. Survival was estimated as the ratio of the signal measured in treated cells relative to untreated control.

In cultured wound healing assays MCF-7 untreated or pre-treated for 4 days with GKS126 were grown to 100% confluence. A 1000 µL sterile pipette tip was used to produce a scratch in the monolayer of cells. Standard cell media was change to media containing 1% of FBS and supplemented or not with GSK126. Cells were allowed to close the wound for 48 hours. The area of the wound was imaged every 24 hours using a widefield microscope and quantified using Image J software. The area of the wound at each time point was normalized to the area of the wound at time zero.

RT-qPCR

For RT-qPCR, RNA was isolated using Trizol reagent (Thermofisher), reverse transcribed using RevertAid Frist Strand cDNA systhesis kit (Thermofisher) and analysed by SYBRG real-time PCR using GoTaq qPCR Master Mix (Promega). Primers used are provided in supplementary table S1.

Western blotting

Western blots of whole cell extracts or histone preparations were carried out using standard procedures as previously described [8]. The following primary antibodies were used: mouse anti-H3K27me3 (Active Motif), rabbit anti-SNAI2 (CST), mouse anti-E-CADHERIN (BD), mouse anti-ACTIN B (Sigma Aldrich). Secondary species-specific antibodies conjugated to horseradish peroxidase were used: anti-rabbit-HRP (GE-Healthcare), anti-mouse-HRP (GE-Healthcare) and anti-goat-HRP (Abcam). Clarity Western ECL reagents (Bio-Rad) was used for detection. More information about antibodies used is provided in supplementary table S1.

ChIPseqs analysis

Public ChIP-seq datasets of H3K27me3 (GSM970218) and H3K4me3 (GSM945269) were analyzed. Aligment of the sequence reads was done using Bowtie2 [18] and human genome hg19 were used for mapping. Unmapped and multimapped reads were filtered out with SAMTools [19] and SamBamba [31] to keep only uniquely aligned sequences. BigWigs were generated after normalizing with their input signal using the BamCompare function of the deepTools suite package [25]. Peak calling was performed with MACS version 3 [33] using the input as background for normalization. Peaks with $p \leq 0.01$ values were considered significant. Significant peaks were annotated with Homer software [10] by defining promoter regions as ±2 kb from the start of the transcription start site (TSS). The coverage of the samples around the TSS was performed with the Bioconductor package coverageView for a genomic window of +- 4kb using a bin size of 10 bp. R version 4.2.2 and RStudio version 2022.7.1.554 was used.

Bioinformatic analysis of breast cancer tumour samples

Information of 1904 breast cancer tumour samples from the Breast Cancer METABRIC dataset were analysed using CBioportal tools. Kaplan Meier survival analysis and the correlation analyses between mRNA levels of EZH2 of selected target genes were performed.

Statistical analyses

Statistical significance ($p<0.05$) was determined by applying a two-tailed non-parametric Mann-Whitney test. Spearman's correlation coefficient was calculated to measure correlation among variables. All analyses were performed with GraphPad prism 9 and/or R or Rstudio.

Author contributions

DL designed and conceptualized the study. AG and DL designed experiments. AG and AM performed experiments. AG analysed experiments. EBR performed bioinformatic analyses. AG and DL wrote the manuscript. DL obtained funding and supervised research.

Funding

The Landeira lab is supported by the Spanish ministry of science and innovation (PID2019-108108-100, EUR2021-122005), the Instituto de Salud Carlos III (IHRC22/00007), the Andalusian regional government (PC-0246-2017, PIER-0211-2019, PY20_00681) and the University of Granada (A-BIO-6-UGR20) grants. Efres Belmonte-Reche is funded by a Maria Zambrano fellowship.

Acknowledgements

We are very grateful to Dr. Maria Jose Serrano, Dr. Sergio Granados-Principal and Dr. Juan Antonio Marchal for providing cell lines. We thank core facilities at GENYO for excellent technical support.

Competing interests

The authors declare no competing interests.

Figure legends

Figure 1. EZH2 represses mesenchymal genes in breast carcinoma cells.

(A) Venn diagram comparing sets of gene promoters displaying enrichment of H3K27me3 or H3K4me3 at their promoter regions by ChIP-seq in MCF-7 cells.
(B) Plots showing the ChIP-seq average binding profile of H3K27me3 and H3K4me3 around the TSS of gene promoters identified in (A) as bivalent (H3K27me3+H3K4me3) or H3K4m3-only.
(C) Gene Ontology analysis of bivalent genes identified in (A).
(D) Genome browser view of H3K4me3 and H3K27me3 binding profiles at the *SNAI2* locus in MCF-7 cells.
(E) Schematic diagram of the treatment of MCF-7 cells with EZH2i (upper panel). Lower panel shows western blot analysis of whole-cell extracts comparing the level of H3K27me3 during the experiment. ACTIN B provides a loading control.
(F) Analysis of *N-CADHERIN* mRNA expression by RT-qPCR during EZH2i treatment in MCF-7cells. Expression is calculated relative to housekeeping genes *GAPDH* and *ACTINB*.
(G) Analysis of EMT-TFs mRNA expression by RT-qPCR during EZH2i treatment in MCF-7cells. Expression is calculated relative to housekeeping genes *GAPDH* and *ACTINB*.
(H) Western blot analysis of SNAI2 in whole-cell extracts from EZH2i-treated MCF-7 cells. ACTIN B was used as a loading control.
(I) Brightfield images and quantification of cultured wound healing assays using MCF-7 cells that have been treated or not with EZH2i for four days.
(J) Histograms showing the level of expression of mesenchymal genes in indicated cell lines treated or untreated with EZH2i conditions for 14 days.
Mean and SEM of 3 experiments are shown in F, G and J. Asterisks indicate statistical significance using a Mann-Whitney test (* $p<0.05$).

Figure 2. EZH2 is required to repress mesenchymal genes during TGF-β-dependent MET in MCF-7 cells.

(A) Schematic diagram of the experimental conditions used to study the inhibition of EZH2 activity (EZH2i 5 µM) during reversible EMT-MET (TGF-β + EGF).
(B) RT-qPCR analysis showing mRNA level of indicated epithelial (black) and mesenchymal (red) genes during EMT-MET in the absence or presence of EZH2i. Expression level is calculated relative to *GAPDH* and *ACTIN B*.
(C) Brightfield images and histogram analyzing the effect of EZH2i treatment in wound healing closure after 72 hours, in cells corresponding to day 6 or 12 during the EMT-MET described in (A).
Mean and SEM of 3 experiments are shown in B, D, F and G. Asterisks indicate statistical significance using a Mann-Whitney test (* $p<0.05$).

Figure 3. EZH2 level inversely correlates with the expression of mesenchymal genes, and it is associated with poor prognosis of breast cancer patients.

(A) Heatmaps of Spearman´s correlation between the mRNA of *EZH2* and different subsets of genes in 1904 samples from breast cancer tumours. Subsets of bivalent genes and mesenchymal bivalent genes were identified in figure 1A and 1C. The pattern of a set of randomly selected genes is shown for comparison purposes.
(B) Spearman´s correlation of *EZH2* and *SNAI2* mRNA in 1904 patients of breast cancer. Each dot represents expression values of one breast tumour sample.
(C) Kaplan-Meier plots showing survival probability of 1904 breast cancer patients depending on the level of expression of *EZH2* mRNA.

Figure S1. Treatment of MCF-7 cells with EZH2i promotes downregulation of *E-CADHERIN*.

(A) Table showing bivalent genes classified related to mesenchyme identified in figure 1C.
(B) Growth curve of MCF-7 cells treated with EZH2i versus untreated control.
(C) Histogram show the level of *E-CADHERIN* mRNA expression measured by RT-qPCR during EZH2i treatment in MCF-7 cells. Expression is calculated relative to housekeeping genes *GAPDH* and *ACTINB*.
(D) Western blot analysis of the level of E-CADHERIN in whole-cell extracts from EZH2i-treated MCF-7 cells. ACTIN B was used as a loading control.
(E) Histogram showing cell survival of indicated cells lines treated with EZH2i relative to untreated control after resazurin staining and fluorescence quantification.
(F) Brightfield images of breast cancer cell lines plated at low density in the presence of EZH2i for 14 days.

Figure S2. TGF-β-induced EMT is reversible in MCF-7 cells.

(A) Scheme of the experimental design used to induce EMT-MET in MCF-7 cells.
(B) Analysis of mRNA expression by RT-qPCR of indicated epithelial (black) or mesenchymal (red) genes during EMT-MET. Relative expression level against *GAPDH* and *ACTIN B* is shown.
(C) Brightfield images and quantification plot comparing the wound healing capacity after 72 hours of cells obtained at day 0, 6 and 12 during EMT-MET.

Bibliography

1 Adibfar S, Elveny M, Kashikova HS, Mikhailova MV, Farhangnia P, Vakili-Samiani S *et al*. The molecular mechanisms and therapeutic potential of EZH2 in breast cancer. Life Sciences 2021; 286: 120047.

2 Alford SH, Toy K, Merajver SD, Kleer CG. Increased risk for distant metastasis in patients with familial early-stage breast cancer and high EZH2 expression. Breast Cancer Research and Treatment 2012; 132: 429-437.

3 Blackledge NP, Klose RJ. The molecular principles of gene regulation by Polycomb repressive complexes. Nature reviews Molecular cell biology 2021.

4 Bracken AP, Kleine-Kohlbrecher D, Dietrich N, Pasini D, Gargiulo G, Beekman C *et al*. The Polycomb group proteins bind throughout the *INK4A-ARF* locus and are disassociated in senescent cells. Genes & Development 2007; 21: 525-530.

5 Comet I, Riising EM, Leblanc B, Helin K. Maintaining cell identity: PRC2-mediated regulation of transcription and cancer. Nature Reviews Cancer 2016; 16: 803-810.

6 Dongre A, Weinberg RA. New insights into the mechanisms of epithelial–mesenchymal transition and implications for cancer. Nature Reviews Molecular Cell Biology 2019; 20: 69-84.

7 Flavahan WA, Gaskell E, Bernstein BE. Epigenetic plasticity and the hallmarks of cancer. Science 2017; 357: eaal2380.

8 Gallardo A, Molina A, Asenjo HG, Martorell-Marugan J, Montes R, Ramos-Mejia V *et al*. The molecular clock protein Bmal1 regulates cell differentiation in mouse embryonic stem cells. Life Sci Alliance 2020; 3.

9 Gallardo A, Molina A, Asenjo HG, Lopez-Onieva L, Martorell-Marugán J, Espinosa-Martinez M *et al*. EZH2 endorses cell plasticity to non-small cell lung cancer cells facilitating mesenchymal to epithelial transition and tumour colonization. Oncogene 2022.

10 Heinz S, Benner C, Spann N, Bertolino E, Lin YC, Laslo P *et al*. Simple combinations of lineage-determining transcription factors prime cis-regulatory elements required for macrophage and B cell identities. Molecular cell 2010; 38: 576-589.

11 Hirukawa A, Smith HW, Zuo D, Dufour CR, Savage P, Bertos N *et al*. Targeting EZH2 reactivates a breast cancer subtype-specific anti-metastatic transcriptional program. Nature Communications 2018; 9: 2547.

12 Jacobs JJL, Kieboom K, Marino S, DePinho RA, van Lohuizen M. The oncogene and Polycomb-group gene bmi-1 regulates cell proliferation and senescence through the ink4a locus. Nature 1999; 397: 164-168.

13 Jang S-H, Lee JE, Oh M-H, Lee J-H, Cho HD, Kim K-J *et al*. High EZH2 Protein Expression Is Associated with Poor Overall Survival in Patients with Luminal A Breast Cancer. Journal of Breast Cancer 2016; 19: 53.

14 Katsuno Y, Derynck R. Epithelial plasticity, epithelial-mesenchymal transition, and the TGF-β family. Developmental Cell 2021; 56: 726-746.

15 Kim KH, Roberts CWM. Targeting EZH2 in cancer. Nature Medicine 2016; 22: 128-134.

16 Kleer CG, Cao Q, Varambally S, Shen R, Ota I, Tomlins SA *et al*. EZH2 is a marker of aggressive breast cancer and promotes neoplastic transformation of breast epithelial cells. Proceedings of the National Academy of Sciences 2003; 100: 11606-11611.

17 Lambert AW, Pattabiraman DR, Weinberg RA. Emerging Biological Principles of Metastasis. Cell 2017; 168: 670-691.

18 Langmead B, Salzberg SL. Fast gapped-read alignment with Bowtie 2. Nature methods 2012; 9: 357-359.

19 Li H, Handsaker B, Wysoker A, Fennell T, Ruan J, Homer N *et al*. The Sequence Alignment/Map format and SAMtools. Bioinformatics 2009; 25: 2078-2079.

20 Lüönd F, Sugiyama N, Bill R, Bornes L, Hager C, Tang F *et al*. Distinct contributions of partial and full EMT to breast cancer malignancy. Developmental Cell 2021; 56: 3203-3221.e3211.

21 Macrae TA, Fothergill-Robinson J, Ramalho-Santos M. Regulation, functions and transmission of bivalent chromatin during mammalian development. Nature reviews Molecular cell biology 2022.

22 McCabe MT, Ott HM, Ganji G, Korenchuk S, Thompson C, Van Aller GS *et al*. EZH2 inhibition as a therapeutic strategy for lymphoma with EZH2-activating mutations. Nature 2012; 492: 108-112.

23 Pal A, Barrett TF, Paolini R, Parikh A, Puram SV. Partial EMT in head and neck cancer biology: a spectrum instead of a switch. Oncogene 2021.

24 Piunti A, Shilatifard A. The roles of Polycomb repressive complexes in mammalian development and cancer. Nature Reviews Molecular Cell Biology 2021; 22: 326-345.

25 Richter AS, Ryan DP, Kilpert F, Ramírez F, Heyne S, Manke T *et al*. deepTools2: a next generation web server for deep-sequencing data analysis. Nucleic acids research 2016; 44: W160-W165.

26 Schuettengruber B, Bourbon H-M, Di Croce L, Cavalli G. Genome Regulation by Polycomb and Trithorax: 70 Years and Counting. Cell 2017; 171: 34-57.

27 Serresi M, Gargiulo G, Proost N, Siteur B, Cesaroni M, Koppens M *et al*. Polycomb Repressive Complex 2 Is a Barrier to KRAS-Driven Inflammation and Epithelial-Mesenchymal Transition in Non-Small-Cell Lung Cancer. Cancer Cell 2016; 29: 17-31.

28 Serresi M, Siteur B, Hulsman D, Company C, Schmitt MJ, Lieftink C *et al*. Ezh2 inhibition in Kras-driven lung cancer amplifies inflammation and associated vulnerabilities. The Journal of experimental medicine 2018; 215: 3115-3135.

29 Serresi M, Kertalli S, Li L, Schmitt MJ, Dramaretska Y, Wierikx J *et al*. Functional antagonism of chromatin modulators regulates epithelial-mesenchymal transition. Science Advances 2021; 7: eabd7974.

30 Simeonov KP, Byrns CN, Clark ML, Norgard RJ, Martin B, Stanger BZ *et al*. Single-cell lineage tracing of metastatic cancer reveals selection of hybrid EMT states. Cancer Cell 2021; 39: 1150-1162.e1159.

31 Tarasov A, Vilella AJ, Cuppen E, Nijman IJ, Prins P. Sambamba: fast processing of NGS alignment formats. Bioinformatics (Oxford, England) 2015; 31: 2032-2034.

32 Yomtoubian S, Lee SB, Verma A, Izzo F, Markowitz G, Choi H *et al*. Inhibition of EZH2 Catalytic Activity Selectively Targets a Metastatic Subpopulation in Triple-Negative Breast Cancer. Cell Reports 2020; 30: 755-770.e756.

33 Zhang Y, Liu T, Meyer CA, Eeckhoute J, Johnson DS, Bernstein BE *et al*. Model-based analysis of ChIP-Seq (MACS). Genome biology 2008; 9: R137.

34 Zhang Y, Donaher JL, Das S, Li X, Reinhardt F, Krall JA *et al*. Genome-wide CRISPR screen identifies PRC2 and KMT2D-COMPASS as regulators of distinct EMT trajectories that contribute differentially to metastasis. Nature Cell Biology 2022; 24: 554-564.

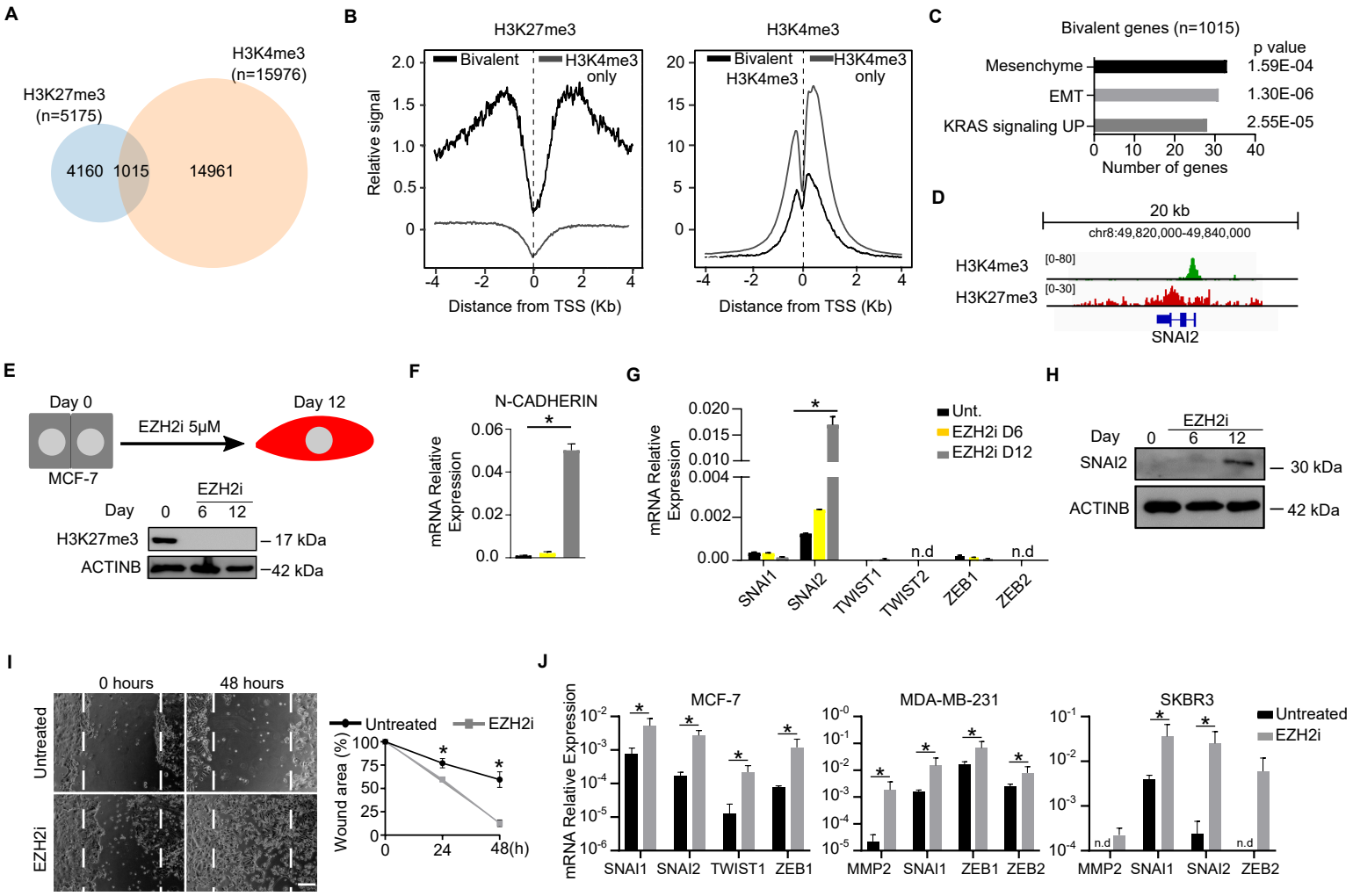
A
H3K27me3
(n=5175)
H3K4me3
(n=15976)
4160
1015
14961
B
H3K27me3
H3K4me3
Bivalent
H3K4me3 only
Relative signal
Distance from TSS (Kb)
C
Bivalent genes (n=1015)
p value
Mesenchyme
EMT
KRAS signaling UP
1.59E-04
1.30E-06
2.55E-05
Number of genes
D
20 kb
chr8:49,820,000-49,840,000
H3K4me3
H3K27me3
[0-80]
[0-30]
SNAI2
E
Day 0
Day 12
EZH2i 5μM
MCF-7
EZH2i
Day 0 6 12
H3K27me3
ACTINB
17 kDa
42 kDa
F
N-CADHERIN
mRNA Relative Expression
G
Unt.
EZH2i D6
EZH2i D12
n.d
SNAI1
SNAI2
TWIST1
TWIST2
ZEB1
ZEB2
H
EZH2i
Day 0 6 12
SNAI2
ACTINB
30 kDa
42 kDa
I
0 hours
48 hours
Untreated
EZH2i
Wound area (%)
48(h)
J
MCF-7
MDA-MB-231
SKBR3
mRNA Relative Expression
Untreated
EZH2i
SNAI1
SNAI2
TWIST1
ZEB1
MMP2
ZEB2
n.d

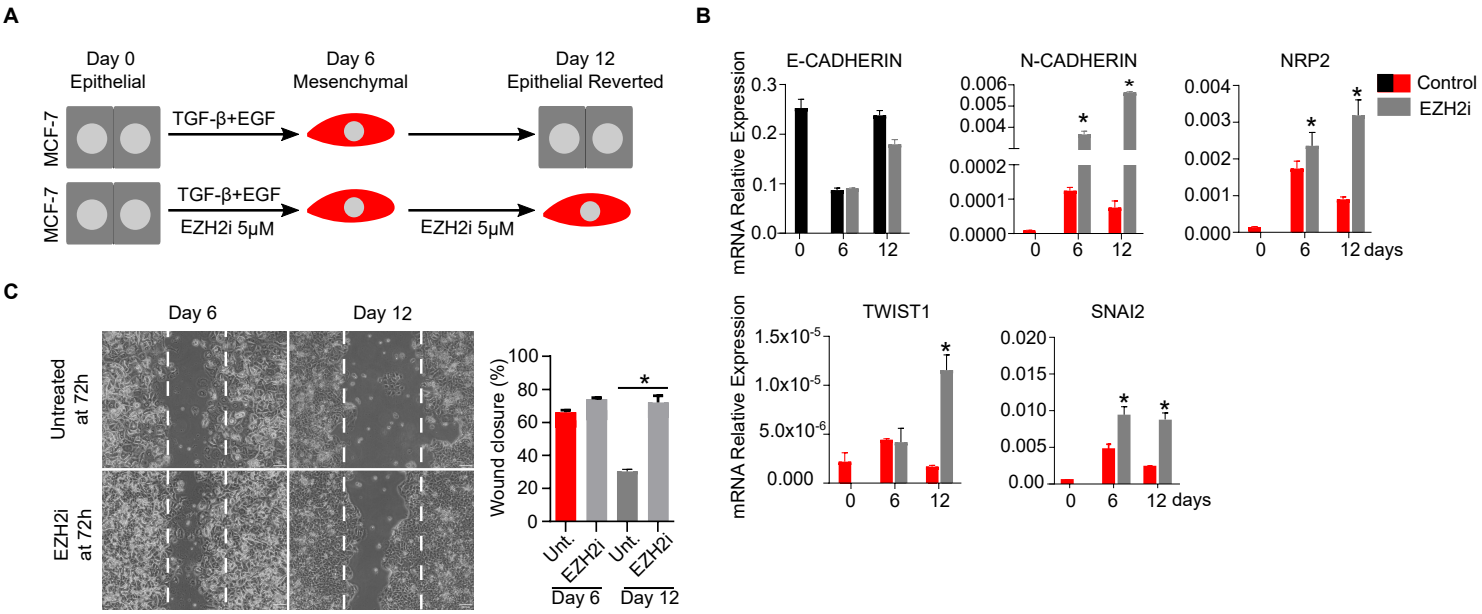
A
Day 0
Epithelial
Day 6
Mesenchymal
Day 12
Epithelial Reverted
MCF-7
TGF-β+EGF
MCF-7
TGF-β+EGF
EZH2i 5μM
EZH2i 5μM
B
E-CADHERIN
N-CADHERIN
NRP2
Control
EZH2i
mRNA Relative Expression
0 6 12
0 6 12 days
TWIST1
SNAI2
C
Day 6
Day 12
Untreated at 72h
EZH2i at 72h
Wound closure (%)
Unt.
EZH2i
Day 6
Day 12

Figure 3

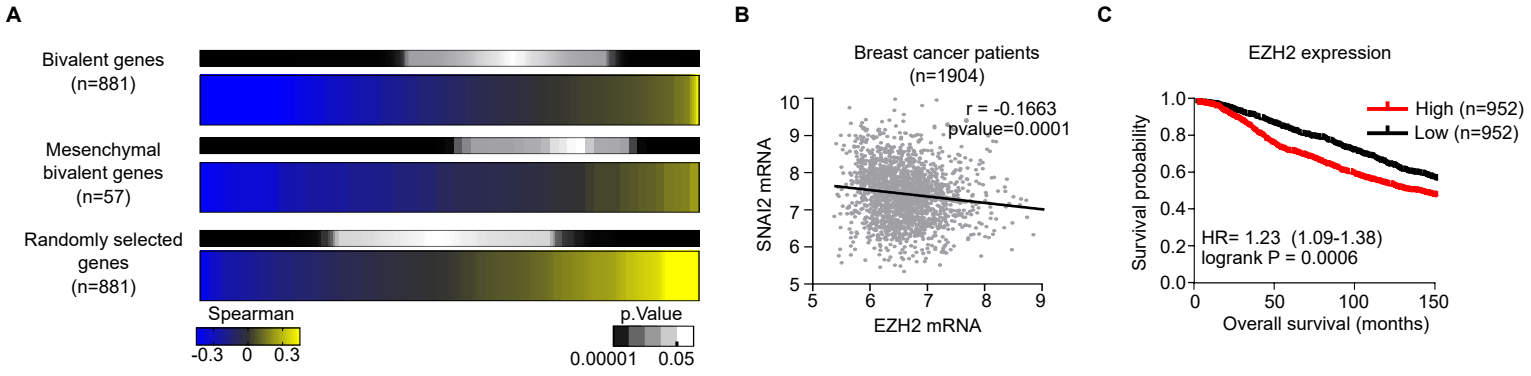
A
Bivalent genes
(n=881)
Mesenchymal
bivalent genes
(n=57)
Randomly selected
genes
(n=881)
Spearman
-0.3 0 0.3
p.Value
0.00001 0.05
B
Breast cancer patients
(n=1904)
r = -0.1663
pvalue=0.0001
SNAI2 mRNA
EZH2 mRNA
C
EZH2 expression
High (n=952)
Low (n=952)
HR= 1.23 (1.09-1.38)
logrank P = 0.0006
Survival probability
Overall survival (months)